Experimental Study on the Effects of Liquid Cross Flow on the Submerged Gas Jet

Ping Dong[1,2,a], Shaofeng Gong[1,2], Bingju Lu[1,2], Liping Qin[1,2], Shiping Zhao[1,2] and Dong Cheng[1,2]

[1]The 713 Research Institute of CSIC, ZhengZhou 450015, China
[2]Henan Key Laboratory of Underwater Intelligent Equipment, ZhengZhou 450015, China
a. dongping@mail.ustc.edu.cn

Keywords: Liquid cross flow, gas jet, penetration length, multi-phase flow.

Abstract: The interaction between the gas jet and liquid cross flow is not well characterized for the difficulties in experimental performance. In this paper, a new experimental facility was designed and the evolution of the gas jet in liquid cross flow was captured by the high speed photography. Five experimental cases with different initial liquid cross flow velocities (0.35 m/s, 0.7 m/s, 1.0 m/s, 1.5 m/s, 2.0 m/s) were performed where the momentum ratio of the initial gas jet to liquid cross flow varies to highlight the effects of the liquid cross flow velocity on the flow characteristics. The gas jet morphology and the gas liquid interface were clearly identified from the experimental results, which showed that the gas jet deflected in a less pronounced manner with less unsteadiness generated at the gas liquid interface as the liquid cross flow velocity decreases. Empirical correlations were proposed to predict the characteristic parameters of the submerged gas jet in liquid cross flow.

1. Introduction

A complex flow system is formed when a gas jet is injected into a cross flow. Gas or liquid jet subjected to gaseous cross flow has been widely studied for its importance in many scientific and engineering areas. For example, transverse injection of a liquid fuel jet into a gaseous cross flow is an approach which is often employed in both aviation and stationary power generation systems where rapid fuel penetration, vaporization, mixing of vapor/air and ignition, and consequently sustained combustion process are desired. This method of liquid fuel/gas mixture preparation enhances flame stabilization, fuel conversion efficiency, and accordingly emissions reduction[1,2,3]. Understanding the mechanism of the interaction between the gas jet and gaseous cross flow is crucial to improving the thrust vector control[4], and the performance of the applications related to environmental problems such as the waste gas plume or liquid effluent in stream. Recently, reviews about a gas jet in a gaseous cross flow [5,6], and liquid jet in a gaseous cross flow[7,8] have been presented.

While for the case of gas jet in liquid cross flow, the interaction process and flow structure between the gas jet and liquid cross flow are radically different considering the discrepancy in the density and compressibility between the gas jet and the liquid cross flow. The focus of the present study lies on the injection of a gas jet into a liquid cross flow, which has broad application in

underwater jet propulsion[9], underwater cutting[10] and gas layer drag reduction (GLDR)[11]. An experimental research by Harby et al. [12,13] revealed the development of gas jets submerged in the liquid, and the effects of the Froude number and the nozzle diameter were also studied. Hoefele and Brimacombe carried out high speed photography and pressure measurement of gas discharging into liquids[14]. A recent relevant research by Mäkiharju et al.[11] presented gas jet injection through a circular nozzle beneath a ship hull in the water, and the topology of the gas jet was studied. The interaction of a gas jet and liquid cross flow creates a typical complex flow-field as depicted in Fig. 1, and the whole gas jet injection consists of jet regime region, a transition regime region, a plume regime region, shear layer and entrainment zone.

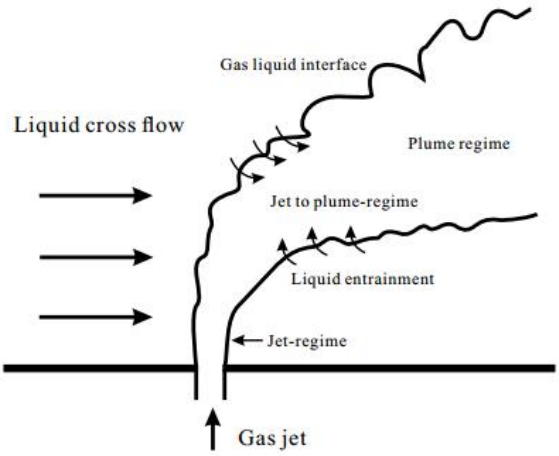

Figure 1: Submerged gas jet into a liquid cross flow.

2. Experimental Devices

The experiments were performed by an experimental facility as shown in Figure 2. The whole experimental system consists of three subsystems including the experimental basin (providing the liquid ambient), the movable injector system which generated the gas jet and the cross flow velocity, and the imaging system.

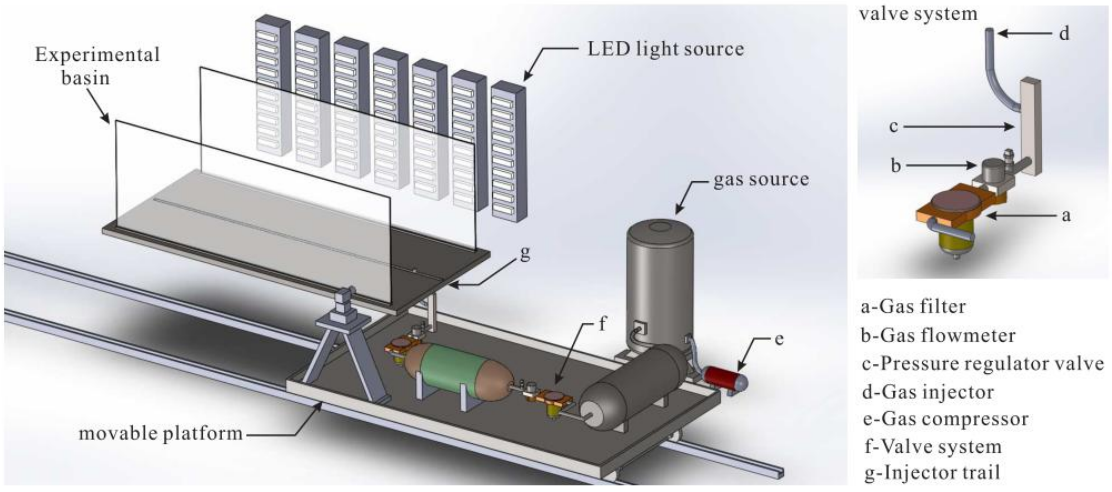

Figure 2: Schematic diagram of the experimental set-up.

2.1. Moveable Injector System

The initial gas jet and accurate incoming flow condition are crucial to perform the experiments, and in the present experimental facility, a movable injector system is elaborately designed to satisfy the experimental requirement. Constant mass flow rate to the injector was sustained by a gas source equipped with a valve system which is insensitive to the back pressure changes. A gas tank in conjunction with an air compressor was designed to supply a 6m3 reservoir maintained at the fixed demanded pressure. Dried air was used as the gas source, and the moveable injector system should move stably along the track at the demand velocity.

2.2. Experimental Basins

The experimental basin is located at the underwater laboratory in the 713 Research institute of CSIC, and the scale of the basin is 80 m in length and 6.5 m in width and 12 m in depth (The depth of the water can be adjusted according to the experimental condition). An automatic carriage transports instruments beneath the bottom of the basin at speeds ranging from 0.1 m/s to 5 m/s. The test section of the basin is made of transparent material which provides the situation for flow visualization and optical measurements. There are tracks under the experimental basin along which the movable injector system operates. Before each of the tests, a period of time interval (about half an hour) is taken to guarantee the initial condition of the ambient liquid.

2.3. Imaging System

The imaging system including a Photron FASTCAM APS-RX with a Canon lens (EF 24-30 mm, f/28L II USM) was fixed on the injection system to move synchronously with the injector system. The height of the camera and the distance from the experimental section can be adjusted according to the experimental situations. The illumination system composed of a series of 100 W light-emitting diode (LED) lights provides the optical conditions. Each of the experiments was recorded for at least for 5 seconds with 1024×860 pixel resolution at 200 Hz frame rate and 5 ms exposure time.

2.4. Experimental Test Conditions

The operation conditions for the experiments are listed in Table 1. The independent parameters of the experimental consisted of the free-stream flow speed, $U\infty$, diameters of the gas injection nozzle exit, dN, mass flow rate of the jet, mi, ambient static pressure, $P\infty$, and the depth of the water, h. The density of the air ρj was equal to 1.2 kg/m−3 at the ambient pressure and temperature, and the density of the liquid water $\rho\infty$, was assumed to be constant throughout the experiment and equaled to 998 kg/m−3. The Mach number was defined in the gas phase only at the exit plane of the nozzle. The stagnation pressure before the nozzle was sustained at about 1.26 × 106 Pa, and the pressure at the nozzle exit was 2.25 × 105 Pa. The Mach number was about 1.78 with a uncertain of ± 0.02 for all the cases. The temperature of the water was sustained at about 283 K during the experiments.

Table 1: Experimental Parameters for all Cases.

Parameters	Range	Uncertainty	Description
U∞	0.2 m/s to 2m/s	± 0.5%	Velocity of the liquid cross flow
dN	12 mm	±0.1 mm	Nominal inner diameter
mi	0.165 kg/s	± 1.5%	Mass flow rate of the nozzle
P∞	101× 105 Pa	± 2.5%	Ambient pressure
h	10 m	± 3.0%	Water depth

3. Experimental Results and Analysis

The morphologies of the gas jets with liquid cross flow velocities ranging from 0.35 m/s to 2 m/s are illustrated in Figure 3. For all cases, the trajectory of gas jet is deflected by the liquid cross flow, and the gas jet deflected in a less pronounced manner with less unsteadiness generated at the gas liquid interface as the liquid cross flow velocity decreases. To achieve the space and time averaging morphologies of the gas jet, all the experimental results were processed by two methods included in a MATLAB program, namely the summation and statistical methods. Firstly, the raw experimental image was digitized based on a threshold pixel intensity to define the interface between the gas phase and the ambient liquid, and thus the edges of the gas jets can be defined. Secondly, the digitized images were summed and averaged to get time and space average morphologies of the gas jet in the summation method, and the parameters were extracted from the time and space average images. The summation images of the experimental results are depicted in Figure 4. In the statistical method, parameters were extracted from each image and summed and averaged statistically for all frames from each experiment. Generally, as will be shown in the subsequent sections the results achieved by the two methods seem to be in good agreement.

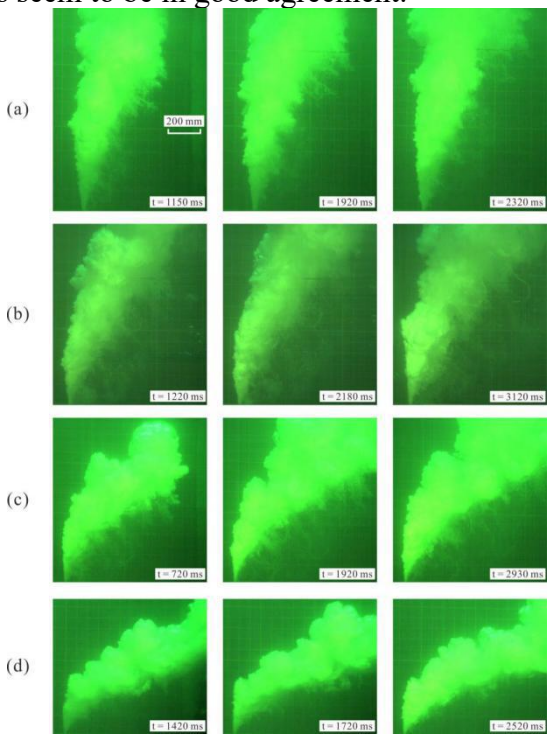

Figure 3: Experimental results of case submerged gas jet with liquid cross flow velocity (a) 0.35 m/s, (b) 0.70 m/s, (c) 1.0 m/s, (c) 2.0 m/s.

As a gas jet is injected into a liquid ambient with cross velocity, the flow structures and the process are essentially unsteady and turbulent, and the static pressure of the water makes the flow complicated by involving oscillating release of the gas. In the near nozzle exit region, the gas jet is mainly dominated by the gas jet momentum and obvious spreading process occurs. The effects of the liquid cross flow on the gas jet are dependent on the magnitude of the cross flow velocity. As the gas jet penetrates further, the jet momentum decreases rapidly and the gas jet is dominated by the cross flow and the buoyancy force. For the case with 0.35 m/s cross flow velocity, the gas jet evolves with few effects from the cross flow for the small magnitude of the velocity, and correspondingly the boundary of the gas jet bends slightly. With the increase of the cross flow velocity, the boundary of the gas jet becomes more curved and more fluctuations appears at the gas liquid interface. The location of the gas jet boundaries and centerlines (scaled by LQ, that is a geometric length scale associated with the jet development, and for a round jet is the square root of the nozzle area (Ao) [15], i.e., $L_Q = \sqrt{A_o}$) are depicted in Figure 5, 6 for the upstream boundary, downstream boundary and centerlines respectively, and the symbols denote the result from summation method and the lines from statistical method. it can be observed that the upstream boundaries of all the cases have a similar trajectory in the near exit region (or the region dominated by the gas jet momentum), and beyond this region the boundaries bend more rapidly to the downstream with the increase of the cross flow velocity. The corresponding downstream boundaries and the centerlines show the similar regularity. As the gas jet penetration increases, the curvature of the boundaries decrease for the jet momentum has few effects across this region and the gas jet development is dominated by the liquid cross flow and buoyancy.

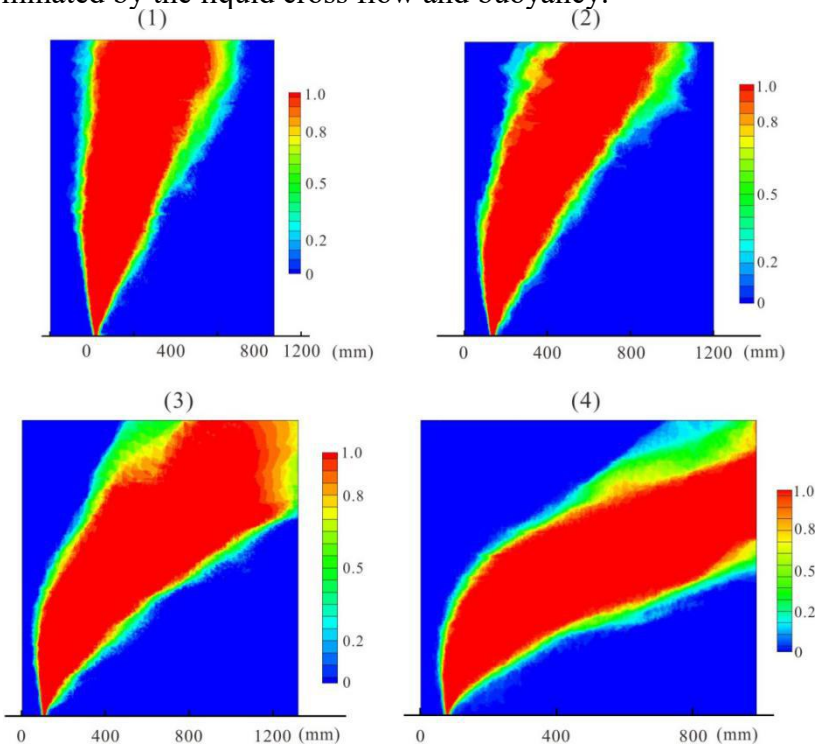

Figure 4: Summation results of submerged gas jets with liquid cross flow velocities (1) 0.35 m/s, (2) 0.70 m/s, (3) 1.0 m/s, (4) 2.0 m/s.

The evolution of the gas jet with liquid cross flow is obviously different from a pure buoyant jet or a vertical gas jet in still water. For those cases, depending on the relative importance of the inertial and buoyancy force the flow can be classified into jet dominated or plume dominated, and the strength of the jet is determined by the value of the jet Froude number which is defined as:

$$Fr_o = \frac{u_o}{\sqrt{g(\Delta\rho/\rho_g)d_N}} \quad (1)$$

In equation (1), u_o stands for the gas velocity at the nozzle exit, g is the gravity acceleration, and $\Delta\rho$ is the density difference between the gas and the ambient liquid, and ρ_g is the density of the gas jet. The effect of the initial momentum on the gas jet increases with the Froude number (Fro), and the jet turns rapidly into a plume as the Fro becomes small enough. Though, in the case of a gas jet with liquid cross flow the relative importance of the coming flow (with velocity U∞) must be taken into consideration.

The first region of the gas jet injected into liquid cross flow is defined as the momentum regime region where the initial momentum related to Froude number determines the flow. The gas jet momentum length denoted as Lm was defined as the length along the nozzle centerline from the nozzle exit to the point with the largest image intensity gradient in the summation images (as defined in Figure 6). The relationship between the gas jet momentum length (Lm) and the cross flow velocity (U∞) is depicted in Figure 7. A logarithm fitting of the data yields a relationship as expressed in Eq. 2, for which a coefficient of determination of R2 = 0.93 was obtained.

$$L_m = c_1 - c_2 \ln(U_\infty - c_3) \quad (2)$$

In equation (2), the Lm is in (mm) and the U∞ is in (m/s), and the coefficients c1, c2 and c3 take the value of 446.23, 290.82 and 0.31.

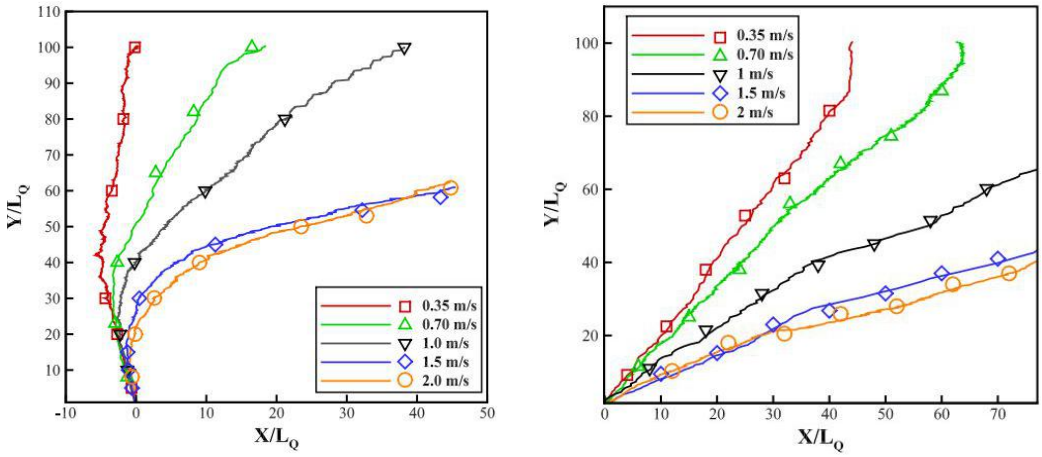

Figure 5: Jet boundaries of the gas jets from summation and statistical methods.

The expansion angles of the underwater gas jets vary with the cross flow velocity. The expansion angles in the upstream (before the centerline) across the near exit region (momentum region) were measured (as φ shown in Figure 6), and the relationship between φ and the cross flow velocity is depicted in Figure 7. Generally the expansion angle decreases with the increase of the cross flow velocity, and rapid decrease appears from case of 0.35 m/s to 1.5 m/s, while for the case of 1.5 m/s and 2 m/s, the decrease of the expansion angles become much slower. Thus, it seems to be that in the near nozzle exit region, the gas jet spreading is primarily influenced by the gas liquid instabilities whose strength is dependent on the magnitude of the cross flow velocity and the initial gas jet parameters (in the present study, the jet parameters are the same for all the case). The interaction of the liquid cross flow and the gas jet enhances the entrainment and instabilities at the gas liquid interface, and therefore exerts a strong influence on the jet-spreading rate.

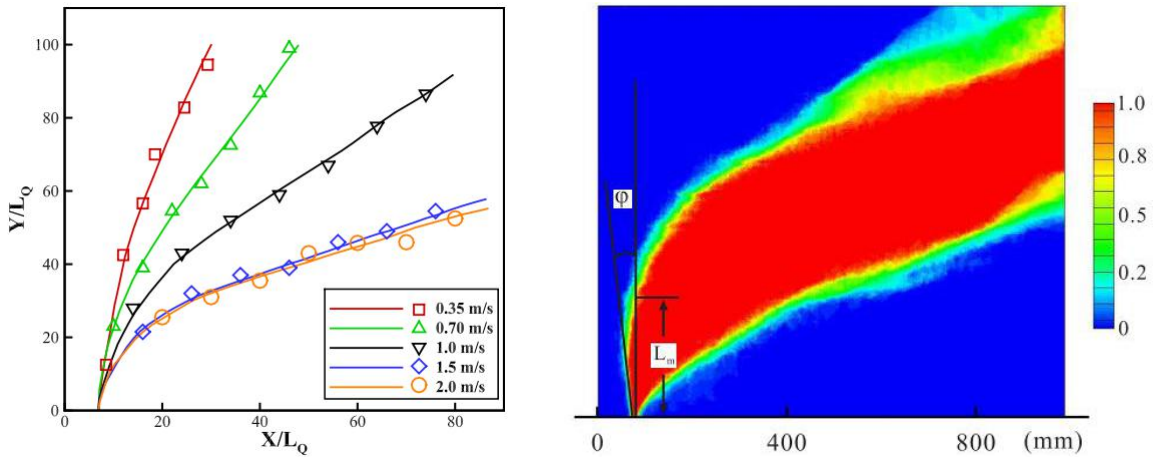

Figure 6: Jet boundaries of the gas jets from summation and statistical methods.

According to the experimental results, an attempt was made to find the relationship between the expansion angle (φ) and the cross flow velocity (U∞) for different cases. Figure 7 shows the expansion angles as a function of the liquid cross flow velocity. It can be seen that the gas jet expansion angles decrease with the liquid cross flow velocity in a nearly logarithmic relationship as expressed in Equqtion 3 with a coefficient of determination of R2 = 0.90,

$$\varphi = c_4 - c_5 \ln (U_\infty - c_6) \quad (3)$$

In equation (3), the cross flow velocity is in (m/s) and the expansion angle is in degree, and c4, c5 and c6 are constants with values of 7.26, 2.3 and 0.1 respectively.

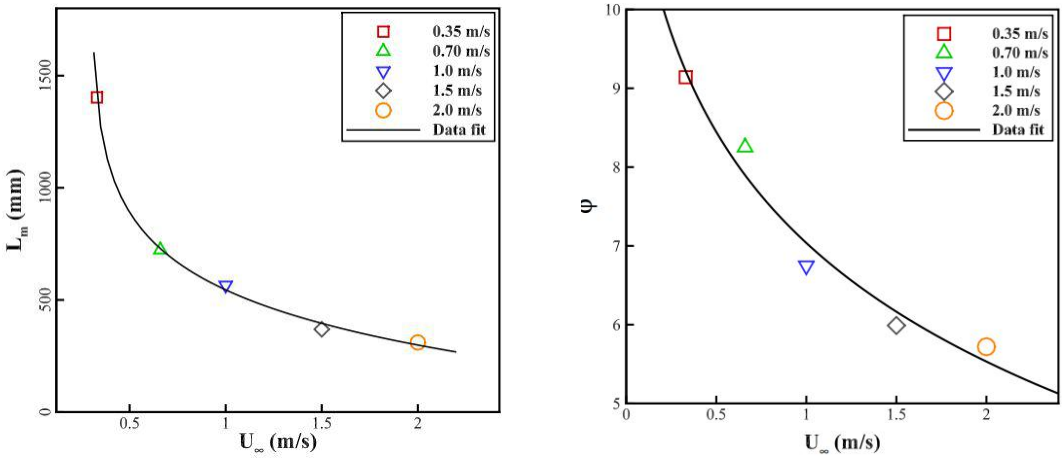

Figure 7: Penetration length and Expansion angle of the gas jets as a function of the liquid cross flow velocity.

4. Conclusion

Experimental study on the submerged gas jet with different liquid cross flow velocities was performed by adopting a newly designed experimental method. Direct measurements of the interfacial morphology of gas jet were performed using the high speed digital photography. It can be concluded that the characteristic structures of the gas jet containing the upstream and downstream boundaries and the centerline are affected by the liquid cross flow, and the magnitude

of the cross flow velocity determines the gas jet development. the expansion angle and the gas jet momentum length follow different logarithmic relationship with the cross flow velocity, and the gas jet width grows linearly in the momentum region. Empirical correlations are proposed to predict the parameters of the gas jet in liquid cross flow.

Acknowledgments

This work was financially supported by the Office of Naval Research under grant JZX7Y20190247021201, program manager Dr F.-Y. Bi. The support from Mr. Ma and Dr. Chen is gratefully appreciated.

References

[1] M. Guo, R. Kishi, B. Shi, Y. Ogata, K. Nishida, Effects of cross-flow on fuel spray injected by hole type injector for direct injection gasoline engine. Atomizat. Sprays 25 (2015), 81–98.

[2] A. Bellofiore, A. Cavaliere, R. Ragucci, Air density effect on the atomization of liquid jets in cross flow. Combust. Sci. Technol. 179 (2007) 319–42.

[3] S. Padala, M. K. Le, S. Kook, E. R. Hawkes, Imaging diagnostics of ethanol port fuel injection sprays for automobile engine applications. Appl. Therm. Eng. 52 (2013), 24–37.

[4] X. Chai, P. S. Iyer, K. Mahesh, Numerical study of high speed jets in crossflow, J. Fluid Mech. 785 (2015) 152–188.

[5] A. R. Karagozian, The jet in crossflow. Phys. Fluids 26 (2014), 101303.

[6] D. R. Getsinger, L. Gevorkyan, O. I. Smith, A. R. Karagozian, Structural and stability characteristics of jets in crossflow. J. Fluid Mech. 760 (2014), 342–67.

[7] M. Broumand, M. Birouk, Liquid jet in a subsonic gaseous crossflow: Recent progress and remaining challenges, Pro. Energ. Combust. Sci. 57 (2016) 1–29.

[8] M. Birouk, N. Lekic, Liquid jet breakup in quiescent atmosphere: a review. Atomizat. Sprays 19 (2009), 501–28.

[9] Y. L. Tang, S. P. Li, Z. Liu, X. Sun, N. F. Wang, Horizontal jet characteristics of an underwater solid rocket motor at the beginning of working. Acta Physica Sinica 64 (2015) 23702.

[10] O. Matsumoto, M. Sugihara, K. Miya, Underwater cutting of reactor core internals by CO laser using local-dry-zone creating nozzle. J. Nuclear Sci. Tech. 29 (1992) 1074–1079.

[11] S. A. Mäkiharju, I. H. R. Lee, G. P. Filip, K. J. Maki, S. L. Ceccio, The topology of gas jets injected beneath a surface and subject to liquid cross-flow, J. Fluid Mech. 818 (2017) 141–183.

[12] K. Harby, S. Chiva, J. L. Muñoz-Cobo, An experimental study on bubble entrainment and flow characteristics of vertical plunging water jets, Exp. Therm. Fluid Sci. 57 (2014) 207–220.

[13] K. Harby, S. Chiva, J. L. Muñoz-Cobo, Modelling and experimental investigation of horizontal buoyant gas jets injected into stagnant uniform ambient liquid, Int. J. Multiphas. Flow 93 (2017) 33-47.

[14] E. O. Hoefele, J. K. Brimacombe, Flow regime in submerged gas injection. Metall. Trans. B 10 (1979), 631–648.

[15] H. L. Ficher, E. J. List, R. C. Koh, N. H. Brooks, Mixing in inland and Coastal Waters, Academic Press, New York, 1979.